

Earthquake Detection Using Accelerometers and Magnetic Sensors

Jack Hunter, Anwar Ali

Abstract—This paper covers the use of accelerometers and magnetic field sensors for detecting an earthquake before it arrives. This is possible because earthquakes emit a small magnetic wave from the epicentre that travels faster than the earthquake itself, allowing early detection and warning. Furthermore, an earthquake is made up of a fast-moving Primary (P) wave, and a slower more dangerous Secondary (S) wave. It is also possible to detect the P wave with an accelerometer to warn of the incoming S wave. The earthquake detection circuit can be constructed using the MPU6050 accelerometer and BMM150 magnetic field sensor, both connected to a Raspberry Pi Pico to utilise its powerful microcontroller that can also connect to an alarm system. This design shows a proof of concept for earthquake detection using magnetic field waves. Nevertheless, there are possible improvements such as using better sensors with less interference as well as progressing into using machine learning for detecting the earthquakes' precursors which could help improve the design further.

Keywords—Earthquakes, epicentre, magnetic field, secondary wave, primary waves.

I. INTRODUCTION

A. Background Knowledge on Earthquakes

EARTHQUAKES are natural disasters that occur all around the globe throughout the year. An earthquake's size is measured on the Richter scale giving a magnitude between 0-10, with larger values resulting in more damage to infrastructure. Earthquakes occur due to pressure built up between tectonic plates, either pushing against each other or rubbing past each other. Over time this pressure builds up until it is released in the form of an earthquake, with the source of the earthquake being called the epicentre. During an earthquake, Primary (P) and Secondary (S) waves are radiated from the epicentre in all directions [1]. P waves travel faster than the S waves but are much less destructive as they are longitudinal waves, thus resulting in only a slight compression of the ground [2]. However, the slower moving S waves are much more dangerous as they are transverse waves, with a much larger amplitude that causes the ground to rise and fall; thus, being the main reason why earthquakes are so destructive. Alongside the physical S and P waves, there is also a magnetic wave that is emitted from the epicentre of the earthquake. This magnetic wave can occur due to piezomagnetic effect, movement of conductive mediums within the earth's crust and the possible displacement between high and low conductive crystal blocks [3].

The magnetic wave produced by an earthquake is in the

Ultra-Low Frequency (ULF) range between 0.001 Hz to 10 Hz [4]. The amplitude of the magnetic wave, measured in Tesla's, is found to be around 1nT with sources varying between 0.7 nT to 1.3 nT [5], [6]. Both its magnitude and frequency are influenced by the strength of the earthquake, with larger earthquakes generally producing stronger and more distinct signals. Comparing the value to the earth's magnetic field, which varies between 22 μ T to 67 μ T, depending on the geographical location, the 1 nT precursor is over four orders of magnitude smaller.

B. Feasibility

The proposed earthquake detection system will detect the magnetic wave from the epicentre of the earthquake before the damaging S waves arrive. This works since the magnetic waves will travel at the speed of light.

$$c = 3 \times 10^8 \text{ m s}^{-1} \quad (1)$$

Furthermore, the ULF magnetic wave attenuates very slowly allowing for it to be picked up by sensors over 100 km away from the epicentre [4]. On the other hand, the S waves travel at around 3 km per second through various minerals within the earth's crust [7]. A simple calculation can find exactly how much time between the magnetic wave being detected and the arrival of the destructive S waves. For example, if the epicentre is 20 km away, the magnetic wave—traveling at the speed of light—will arrive almost instantly, while the S wave will take about 6.7 seconds. This time gap allows a warning signal to be issued, alerting people to the approaching earthquake. Furthermore, P waves travel just faster than S waves at around 5 km per second through various minerals within the earth's crust. Therefore, the P wave will still arrive around 2.6 seconds before the S wave giving a much shorter warning time than from the magnetic signal [8].

A comprehensive block diagram of the earthquake detection system can be seen in Fig. 1. Each earthquake detected circuit would be composed of a power supply, micro controller, magnetometer and a transmitter. In addition to this, protective measures such as current and voltage sensors/regulators and a temperature sensor can be implemented to keep the power output constant. This will also detect if the power supply overheats. Furthermore, multiple earthquake detector circuits can be distributed around areas with high seismic activity allowing for the best chance of early detection. Lastly, each earthquake detection circuit will transmit to a base station when

Jack Hunter and Anwar Ali are with Faculty of Science and Engineering, Swansea University, Swansea UK (e-mail: anwar.ali@swansea.ac.uk).

they detect an incoming earthquake allowing the base station to broadcast a warning alert.

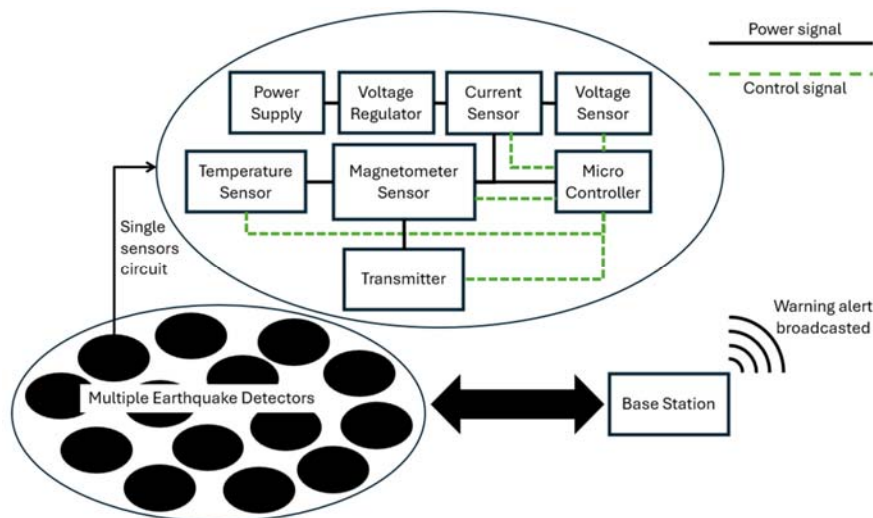


Fig. 1 Wiring schematic for a network of earthquake detection circuits consisting of transmitter, microcontroller, power supply and current, voltage and temperature sensors all linked to a base station

A large bonus to this design is that the detectors can be placed far outside the cities that are vulnerable to earthquakes allowing for the warning signal to be broadcasted even sooner, giving extra warning time. On top of this, the power supply can also be recharged using renewable energy such as solar and/or wind allowing for each detector circuit to be fully self-sufficient.

C. Existing Earthquake Detectors

There are a range of methods for earthquake detection, some of which are aiming to detect the earthquake hours or even days before it happens. These methods rely much more on pattern recognition for precursors, whereas using magnetic field sensors to detect the magnetic waves will result in a shorter warning, but it should be very accurate. These earthquake detectors are incredibly valuable for preventing further damage. One example can be seen when an early earthquake detection system in Japan was triggered and stopped all the trains in the area preventing them being derailed [8]. This was achieved by seismographs detecting the incoming P waves allowing for the trains to come to a safe stop before the S waves arrived [8], [9]. Therefore, on top of the magnetic field sensors, an accelerometer can also be added to the circuit design from Fig. 1, allowing them to detect the P waves and the small tremors they create before the S waves arrive. For this earthquake detection circuit to work, high precision magnetometers and accelerometers will be needed as well as minimal interference and noise from the surroundings. As calculated above, the magnetometer must have a very high resolution and be able to measure all three axes simultaneously, as the earthquake's epicentre could be in any direction. The accelerometer must also be able to measure in all three axes simultaneously and have a high enough resolution to detect the small acceleration due to the P wave tremors from a low magnitude earthquake. All these components must then be able to feedback their

measurements to be compared with predetermined thresholds to determine if an earthquake is inbound.

II. METHODOLOGY

A. Selected Components

The MPU6050 is an accelerometer that can measure all three axes for acceleration as well as function as a gyroscope. The MPU6050 works by using the piezoelectric effect to measure acceleration and rotation in all three directions simultaneously. Furthermore, it is fully compatible using I2C communication with a microcontroller.

The selected magnetometer is the BMM150 that also takes measurements in all three axes simultaneously and supports both SPI and I2C communication allowing it to function with a range of micro controllers. The major downside to this magnetometer is that the resolution is only 0.3 μT , not enough to detect the magnetic wave released by the earthquake. Nevertheless, this circuit will demonstrate proof of the concept for earthquake detection using magnetic sensors.

Both the BMM150 and the MPU6050 are very small (only a few mm wide) integrated circuits (IC) that come attached to a premade printed circuit board (PCB) allowing for a simpler connection between the component and the rest of the circuit. In addition to the accelerometer and the magnetometer, a suitable microcontroller is required to process the sensor's readings. Since both selected components above can communicate via I2C, the Raspberry Pi Pico is a suitable choice for the circuit. It is not only simple to program using MicroPython, but also has two separate I2C channels and a total of 26 GPIO pins, allowing for extra components to be added. Furthermore, it supplies both 5 V and 3.3 V, making it suitable for different components to connect, even if they have different power requirements, such as an OLED screen that requires 3.3

V. This screen will be able to show text, allowing for important information to be displayed, just as if the information was broadcasted to a mobile device. The OLED screen also uses I2C communication with the Pico board. Lastly, some of the extra pins from the Pico board can be used to connect an alarm used to signal when an earthquake is incoming. This can be as simple

as using LEDs and a buzzer to create both a visual and an auditory warning.

B. Circuit Schematic

The circuit wiring schematic for the earthquake detection circuit can be seen in Fig. 2.

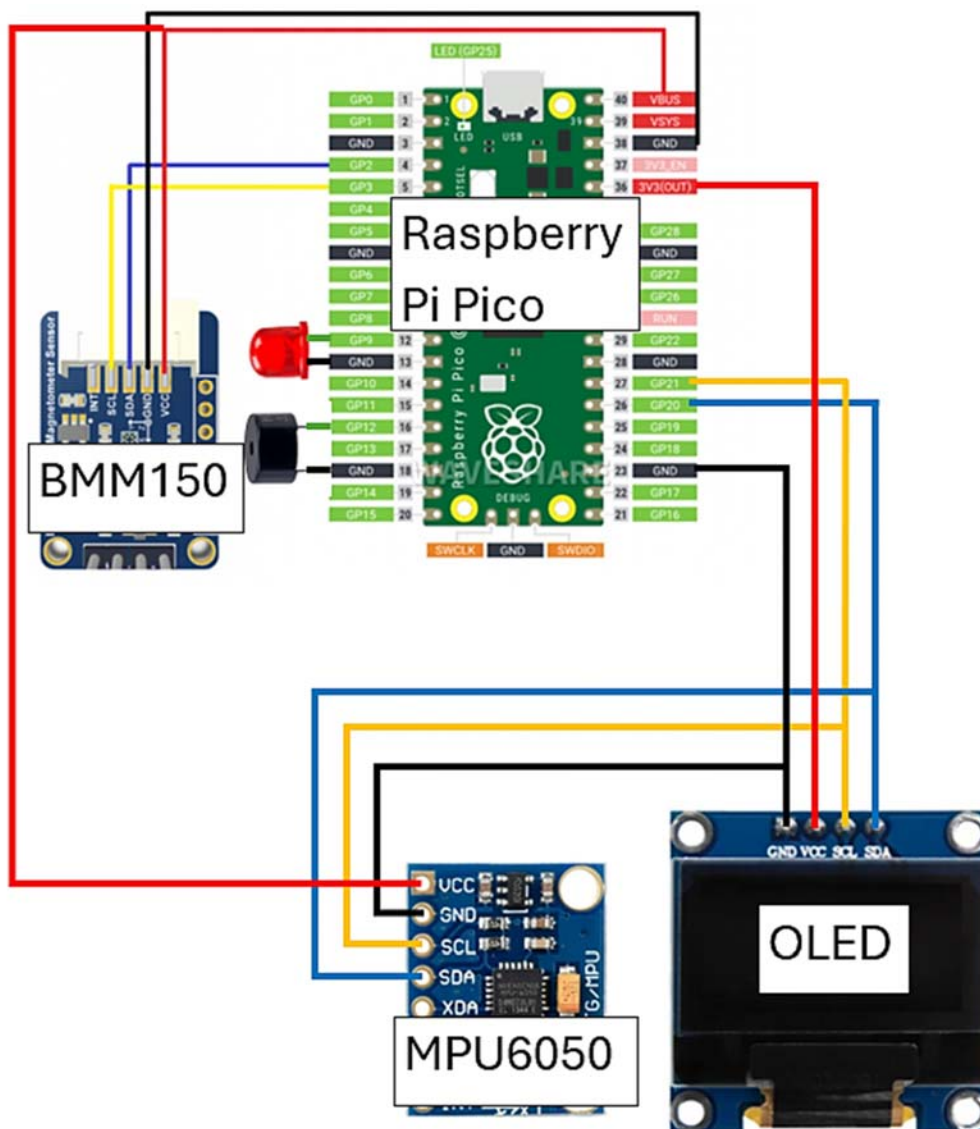


Fig. 2 Colour coded wiring schematic for earthquake detection circuit showing all connections between magnetometer, accelerometer OLED screen and micro controller

The wires seen in Fig. 2 are colour coded, with red being for power connection, black for ground, blue and yellow for SDA and SCL, respectively. The two short green wires are regular GPIO connections between the microcontroller and the alarm, consisting of a buzzer and LED. Importantly, both the BMM150 and MPU6050 can connect to VBUS supplying 5 V from pin number 40 on the Pico board, whereas the OLED must connect to “3V3(OUT)” for the 3.3 V it requires from pin number 36. The other pin numbers are more flexible since all of the ground pins (GND) on the Pico board are internally

connected. Furthermore, the SDA and SCL connection for the BMM150 must be on the I2C channel 1 and GPIO pins 2 and 3, as this is how it is set up within the library that is needed for the magnetometer to function. Both the OLED and MPU6050 can then be attached to the I2C via channel 0 if the hexadecimal addresses are included in the set up for each component. By being on channel 0, the exact pin number for the SDA and SCL connection does not have to be GP20 and GP21, respectively, but as long as the SDA pin number is a multiple of four and the SCL pin number is one larger, it should work the same. Lastly,

the LED and buzzer needs to be connected between any GPIO pin and ground with the correct polarity allowing for them to be toggled between a HIGH and LOW state.

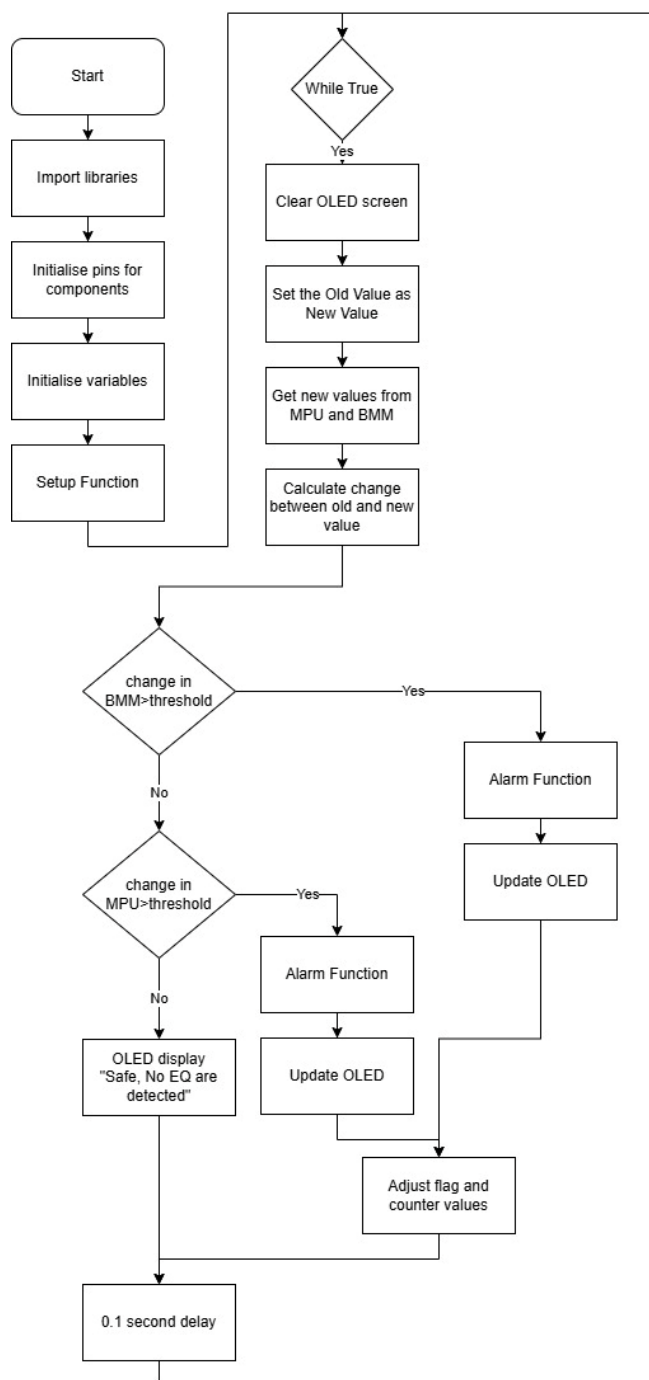


Fig. 3 Flow diagram of code for earthquake detection circuit

C. MicroPython Code

For this circuit to run, the Raspberry Pi Pico needs to be coded to receive information from each sensor and then be able to know whether the threshold for an earthquake is met. This is possible using MicroPython code that is then uploaded to the Pico board using a micro-B USB cable. On top of the written code, multiple premade libraries are needed to allow for various

components to work. Two separate libraries are needed for the MPU6050 to function in addition to both the BMM150 and OLED screen needing a library each too. A flow diagram of the code required for the earthquake detection circuit can be seen in Fig. 3.

There are two main parts to the code, firstly the setup that is used to initialise pins, declare different variables such as counter and flags as well as define different functions that are used throughout the rest of the code. The setup and the functions included are only needed to be run once, before the main loop of code. The other section of the code is the 'while True' loop that runs constantly, checking for incoming magnetic wave fluctuations as well as taking data from the MPU6050 sensor. The method used for detecting an earthquake is to take the most recent value from both the magnetometer and accelerometer and compare them to the previous value. This change is then compared to a pre-set threshold, and when it exceeds the threshold then the alarm function activates. This alarm function simply toggles the buzzer and LED ON and OFF repeatedly, utilising a counter to prevent the function from running forever. Furthermore, upon the threshold being passed, the OLED screen displays text depending upon what sensor measurements triggered the alarm. This is because the BMM150 sensor gives a much longer warning due to the faster speed of the magnetic field wave allowing for the OLED screen to display that an earthquake is inbound. On the other hand, if the change in acceleration exceeds the set threshold, then the OLED screen displays that the earthquake is imminent as there is much less warning due to the shorter time between the P and S wave arriving. After each loop, there is a short delay of 0.1 seconds before the code inside the 'while True' loop is executed again. This small delay is needed to prevent overworking the processor.

D. Setting Thresholds

Setting reasonable thresholds based on earthquake data will allow for the earthquake detection circuit to be working to the best of its ability. Given that the measurements from the MPU and BMM sensors are taken every 0.1 seconds due to the coded delay, the expected change in magnitude with time can be calculated. The magnetic wave produced from the earthquake's epicentre has a magnitude of around 1nT and an ultra-low frequency of approximately 1 Hz [4]-[6]. Therefore, the magnetic field will change by 1 nT every 0.5 s, thus meaning a change of 0.2 nT every 0.1 seconds. As for the physical acceleration changes measured by the MPU6050 accelerometer, the threshold level depends greatly on the magnitude of the earthquake but given that the ideal location for the sensors is far away from any noise or disruption, the threshold can be set quite low, in the range around 0.3 g. This limit is supported by research showing seismic acceleration due to earthquakes to be from 0.001 to 2 g and the P waves will have much less seismic acceleration [10].

III. RESULTS AND DISCUSSION

A. Circuit Results

The constant magnetic strength due to the Earth's poles measured is at $49 \mu\text{T}$ from the BMM150 magnetic sensor and this is constant with the location where the test was conducted. Moving onto the circuit measurements for earthquake detection, the change between the old and new value from the magnetometer has been measured every 0.1 s and can be seen in Fig. 4. This graph was made by constantly measuring the change of the magnetic field strength from the y axis of the BMM150 sensors while physically moving and rotating the sensor. The magnetometer measurements were continuously saved every 0.1 s and recorded in a list. This list has been graphed against time in Fig. 4 alongside the example thresholds.

These thresholds can be seen by the orange and green horizontal lines set at $\pm 25 \mu\text{T}$. This visually shows that the alarm for an incoming earthquake will then activate when the BMM150 sensor measurements exceed this limit, as seen by the vertical red dashed lines.

Due to the location of the circuits' construction and testing being avoidant of tectonic plate boundaries, a real earthquake cannot be observed or measured. Nevertheless, using previous recorded data from other data stations in places with more earthquake activity, the following graph can be made to visualize the expected output. Fig. 5 shows both the magnetic sensor and accelerometer measurements for a theoretical earthquake located approximately 20 km away from the point of measurement.

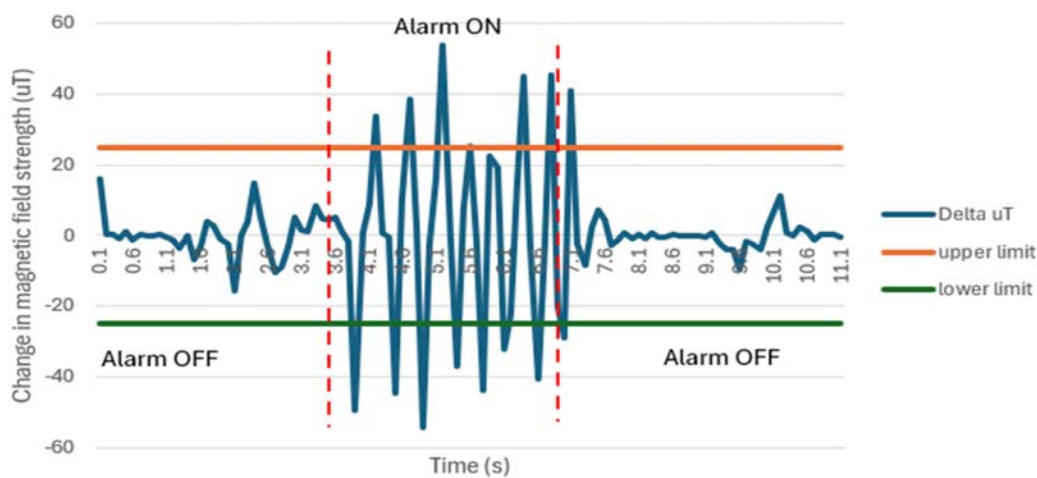


Fig. 4 Change of magnetic field strength with time along with example thresholds visually showing when the alarm is ON and OFF

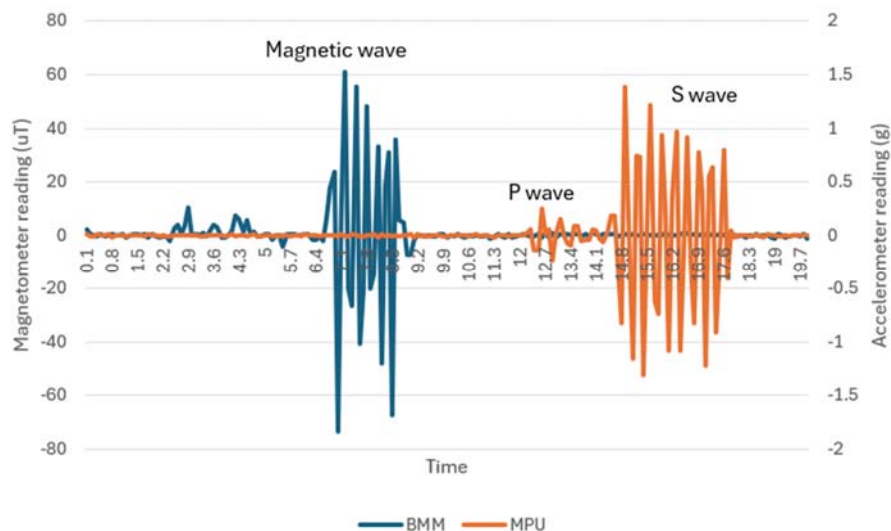


Fig. 5 Theoretical magnetometer and accelerometer signals recorded over time during an earthquake

Fig. 5 shows the magnetic sensors data with the blue trace, with units in μT on the left y axis and the accelerometers data with the orange trace, with units in g on the right y axis. The graph shows the magnetometer reading a large change in the

magnetic field around the 7 second mark, indicating the incoming earthquake. Then, around the 12 second mark, a small tremor is detected from the MPU6050 showing the P wave arriving. Lastly, the slower moving S wave is recorded starting

from the 14 second mark. Fig. 5 clearly shows how the magnetic wave fluctuations can detect an incoming earthquake much sooner than relying upon the accelerometer for the P wave detection.

Within Fig. 5, the units for the magnetometer reading are in micro-Tesla, whereas an actual earthquake gives off waves with an amplitude in nano Tesla's. This is due to the BMM150 sensor picking up extreme amounts of background noise due to local interference from other electronic equipment and devices. Therefore, to give a clear visual of the expected precursors for an earthquake, the predicted magnetic signal seen in Fig. 5 is greatly amplified.

B. Background Noise

The amount of background noise can be recorded by leaving the earthquake detection circuit still and just measuring the BMM150 data. While the measurements always stay consistent

with the expected reading of $49 \mu\text{T}$, looking at the changes between the old and new values shows that despite nothing moving or changing, there is still interference affecting the sensor readings. A graph of the magnetometer noise is shown in Fig. 6. It can be seen that there is always constant interference impacting the magnetometer readings, varying the output by up to $\pm 1.5 \mu\text{T}$. Furthermore, Fig. 6 shows the noise measurements from all three axes showing that they all experience a large amount of interference, especially in the x and z axis. Since even the smallest amount of interference is around $0.2\text{--}0.5 \mu\text{T}$, this shows that the BMM150 does not have the capabilities to be able to accurately detect the magnetic field precursors giving off from an earthquake. This is because the magnetometer will only be able to record down to 200 nT resolution at best, whereas the magnetic field precursor is only around 1 nT , significantly smaller and thus undetectable by the BMM150 sensor.

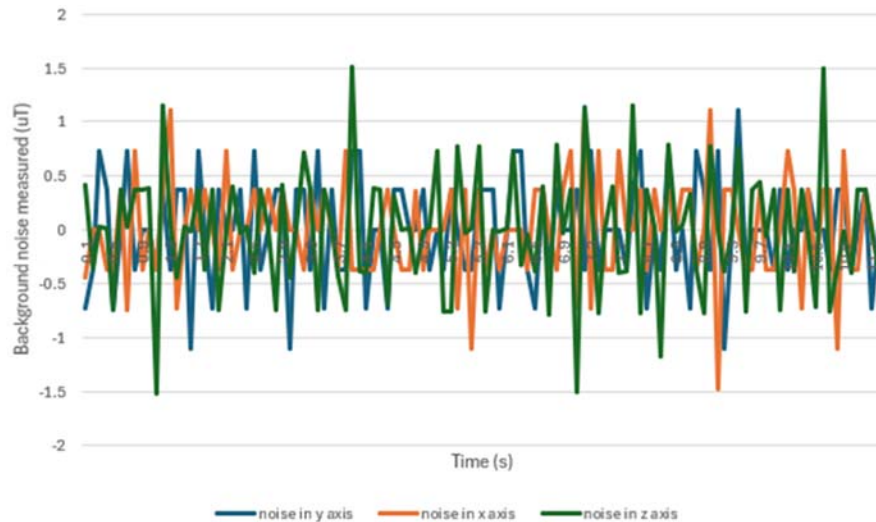


Fig. 6 The noise recorded from the BMM150 on all three axes with time when left at rest measuring background interference

C. Power Loss Analysis

Given that many of these earthquake detector circuits can be used and placed in remote areas, knowing the power consumption is key to making sure they stay in operation. Firstly, the Raspberry pi Pico board will require around 25 mA for constant running, in addition to a further 3.6 mA and 0.5 mA for the MPU6050 and BMM150, respectively. The OLED screen consumes up to 20 mA depending upon how much of the screen is lit up. This gives a total current draw of 49 mA .

Using a 9 V Lithium-ion battery to power the circuit gives 800 mAh of current and thus would power the circuit for slightly over 16 hours. For constant power to the circuit, two batteries can be used, one powering the detection circuit while the other re-charges. The charging time for a Lithium-ion battery is 2 hours from the mains. However, in remote areas where these circuits will be used, a 230 V mains power supply might not be accessible, thus it will rely upon renewable energy such as wind or solar to recharge. This will be heavily dependent upon the location as to how much renewable energy is able to be generated.

On top of this, the Raspberry pi Pico cannot be powered directly by 9 V . This will mean that a buck converter will be required to lower the batteries output voltage to a manageable amount for the Pico. This will require extra power as it is not 100% efficient due to heat losses in components as well as losses due to high switching frequencies. Lastly, the design shown in Fig. 1 uses a transmitter instead of an OLED screen to broadcast the alert for an incoming earthquake. This transmitter will not require power while idle and will only need to draw current while transmitting. This will result in a single 9 V battery lasting even longer than previously calculated since the OLED screen will not be required.

IV. CONCLUSION

Combining the results gathered from the earthquake detection circuit and pre-existing knowledge gained from studying earthquakes, it is possible to detect and emit a warning signal for an incoming earthquake before it arrives. The circuit used to obtain the graphs in Fig. 5, work as proof of concept showing that the magnetic wave created at the epicentre of an

earthquake, if detected, can give a warning much sooner than only relying upon the detection of the P wave. Nevertheless, P wave detection is still a reliable method that can still be used as a second measure, for extra safety. However, using an accelerometer for P wave detection will be less effective when closer to the epicentre as there will be much less time before the S wave arrives. On the other hand, as seen in Fig. 6, a major drawback to the magnetic sensors measurements is the amount of interference from outside sources. This issue of noise only increases further with more electronic equipment around, with each device producing its own electromagnetic waves that hinder the accuracy of the magnetometer.

Possible improvements to the earthquake detection circuit are to use a different magnetometer that has much higher resolution and better noise immunity. One method to help with eliminating the background noise would be to utilise two or more detectors, located nearby to each other, but not too close to cause extra interference. This can allow for the random noise to be compared and reduced, allowing for the earthquakes signal to be more obvious and easier to detect. Another improvement would be to use a transmitter instead of just an LED and buzzer for an alarm. This enhancement would be more effective with a network of earthquake detector circuits, as shown in Fig. 1, where each transmitter can alert a base station to the incoming earthquake, allowing for a much better alarm system to be implemented. This upgraded alarm system could even send a warning message directly to local phones and devices, just like amber alerts for other natural disasters such as tornadoes. Another way to further improve the detection capabilities of the circuit would be to train a machine learning algorithm on the vast amounts of data already recorded about earthquakes. This will also allow for more accurate detection; by not needing to set thresholds as the algorithm can analyse the measured magnetic wave over time to compare both the amplitude and frequency recorded with previously studied data on the go. Furthermore, once the machine learning algorithm is well trained and accurate at earthquake detection, only a few detection circuits will be required as once earthquake precursors are detected, the warning signal can be broadcasted out to a much larger area.

REFERENCES

- [1] Sheriff R, Frederick Windley B. Earth exploration - Seismic refraction methods | Britannica (Internet). www.britannica.com. (cited 2025 Mar 12). Available from: <https://www.britannica.com/topic/Earth-exploration/Seismic-refraction-methods#ref520549>
- [2] Aust A. How Seismic Waves Cause Damage During an Earthquake (Internet). KQED. 2016 (cited 2025 Mar 11). Available from: <https://www.kqed.org/quest/134599/how-seismic-waves-cause-damage-during-an-earthquake>
- [3] Korepanov V. Multi-point measurement system and data processing for earthquakes monitoring (Internet). Ieee.org. 2015 (cited 2025 Mar 13). Available from: <https://ieeexplore.ieee.org/document/7184685>
- [4] Korepanov V. Detection of earthquake magnetic precursors candidates (Internet). Ieee.org. 2024 (cited 2025 Mar 13). Available from: <https://ieeexplore.ieee.org/document/6192444>
- [5] P. Nenovski. Experimental evidence of electrification processes during the 2009 L'Aquila earthquake main shock. Geophysical Research Letters (Internet). 2015 Sep 4 (cited 2025 Mar 13);42(18):7476–82. Available from: <https://arxiv.org/abs/1506.05938>
- [6] Johnston MJS, Mueller RJ, Sasai Y. Magnetic field observations in the

near-field the 28 June 1992 M_w 7.3 Landers, California, earthquake. Bulletin of the Seismological Society of America. 1994 Jun 1;84(3):792–8.

- [7] Compare-Contrast-Connect: Seismic Waves and Determining Earth's Structure | manoa.hawaii.edu/ExploringOurFluidEarth (Internet). manoa.hawaii.edu (cited 2025 Mar 11). Available from: <https://manoa.hawaii.edu/exploringourfluidearth/physical/ocean-floor/layers-earth/compare-contrast-connect-seismic-waves-and-determining-earth-s-structure>
- [8] Zollo A, Amoroso O, Lancieri M, Wu YM, Kanamori H. A threshold-based earthquake early warning using dense accelerometer networks. Geophysical Journal International. 2010 Sep 28;183(2):963–74.
- [9] NEWS K. Tragedy avoided on quake-hit derailed shinkansen from lessons learned (Internet). Kyodo News+. 2022 (cited 2025 Mar 11). Available from: <https://english.kyodonews.net/news/2022/03/afe25e1ac03b-tragedy-avoided-on-quake-hit-derailed-shinkansen-from-lessons-learned.html>
- [10] Accelerometers | EarthScope Primary Instrument Center (Internet). Earthscope.org. 2025 (cited 2025 Apr 15). Available from: <https://epic.earthscope.org/content/instrumentation/sensors/accelerometers>